A Reproducible Asymmetric e926 Activity

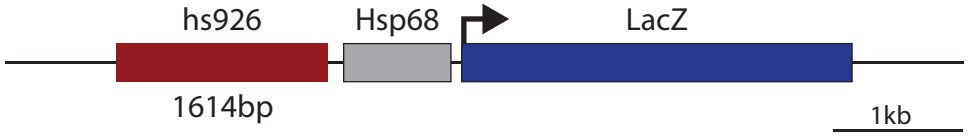

left side
duodenum & stomach
3 of 3 embryos

left side
dorsal mesentery
3 of 3 embryos

right side
aortic sac
2 of 3 embryos

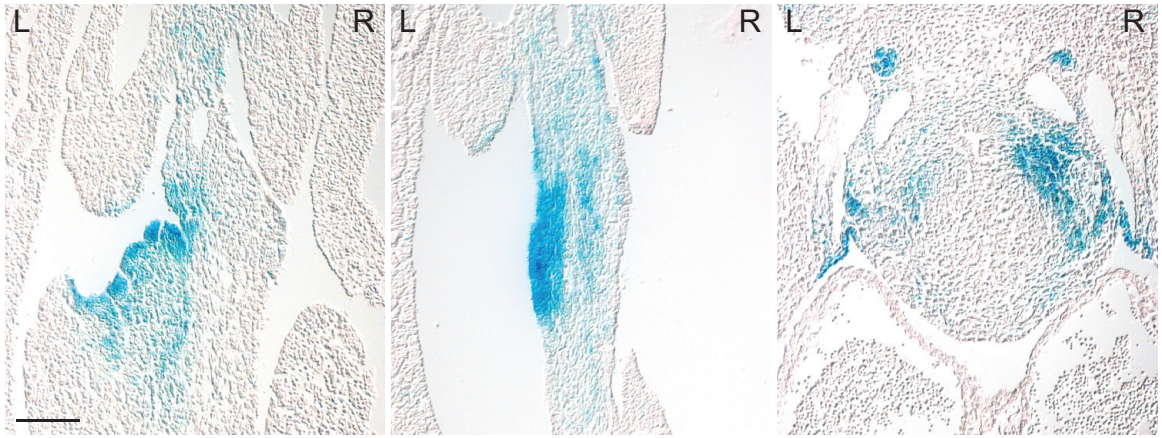

B Conserved PITX2 Motifs in e926

e926 Human:Mouse Conservation

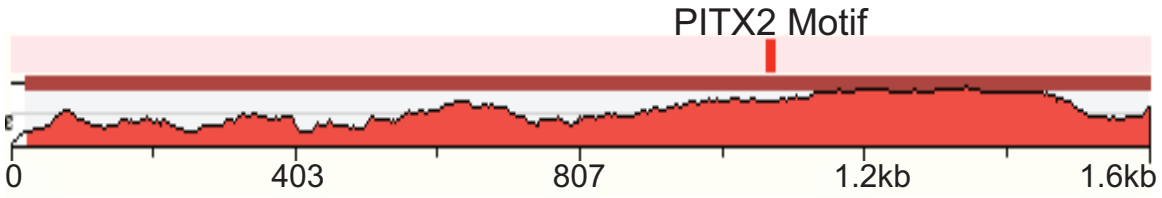

e926 Human:Chicken Conservation

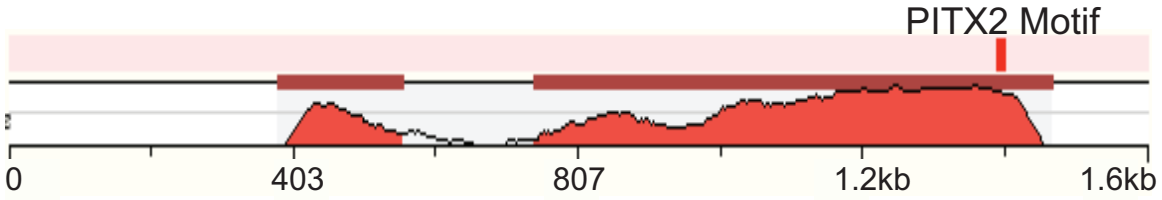

GRO-seq Analysis of *Pitx2* Locus Nascent Transcription

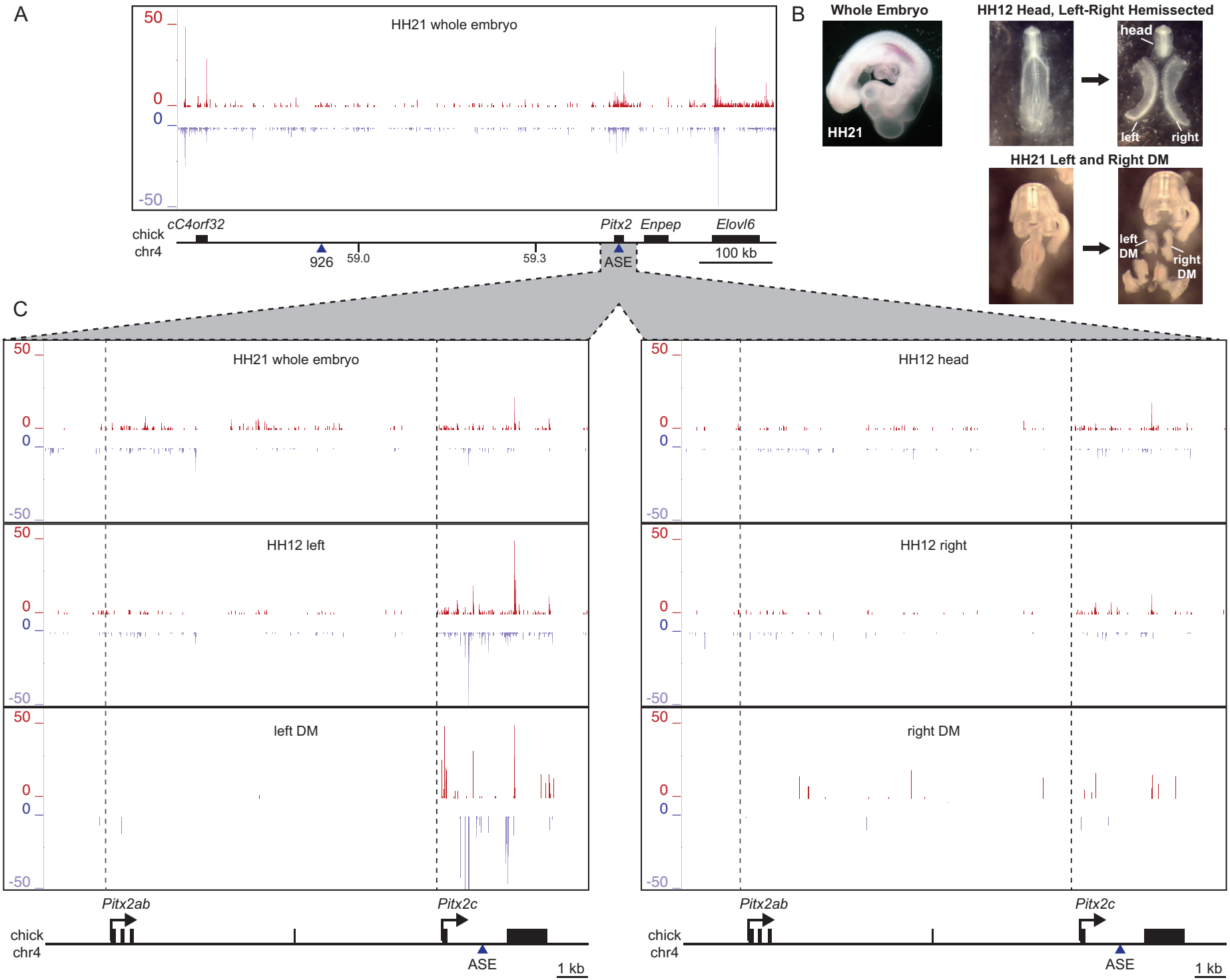

Welsh_FigS3

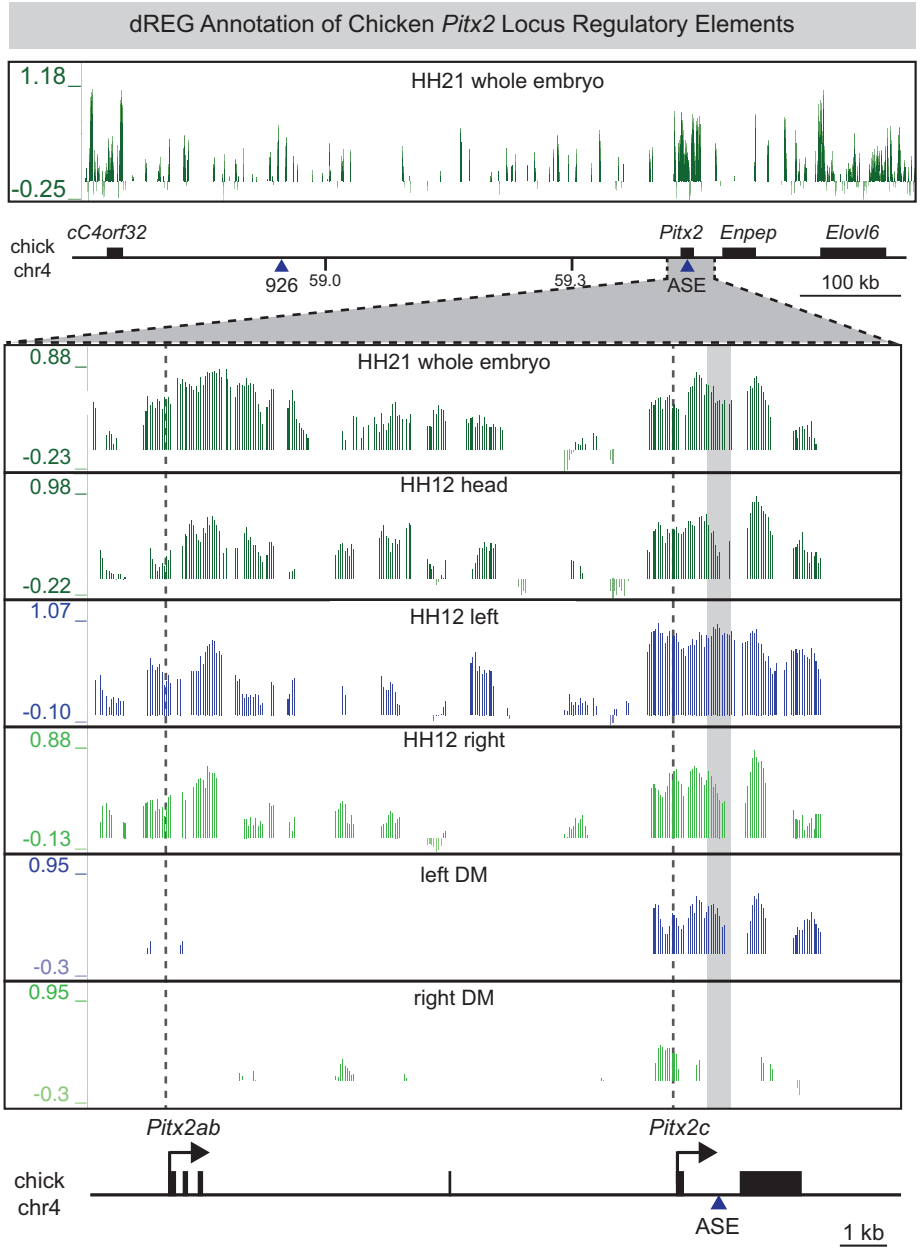
dREG Annotation of Chicken Pitx2 Locus Regulatory Elements
1.18
-0.25
HH21 whole embryo
chick
chr4
cC4orf32
Pitx2
Enpep
Elovl6
926
59.0
59.3
ASE
100 kb
0.88
-0.23
HH21 whole embryo
0.98
-0.22
HH12 head
1.07
-0.10
HH12 left
0.88
-0.13
HH12 right
0.95
-0.3
left DM
0.95
-0.3
right DM
Pitx2ab
Pitx2c
chick
chr4
ASE
1 kb

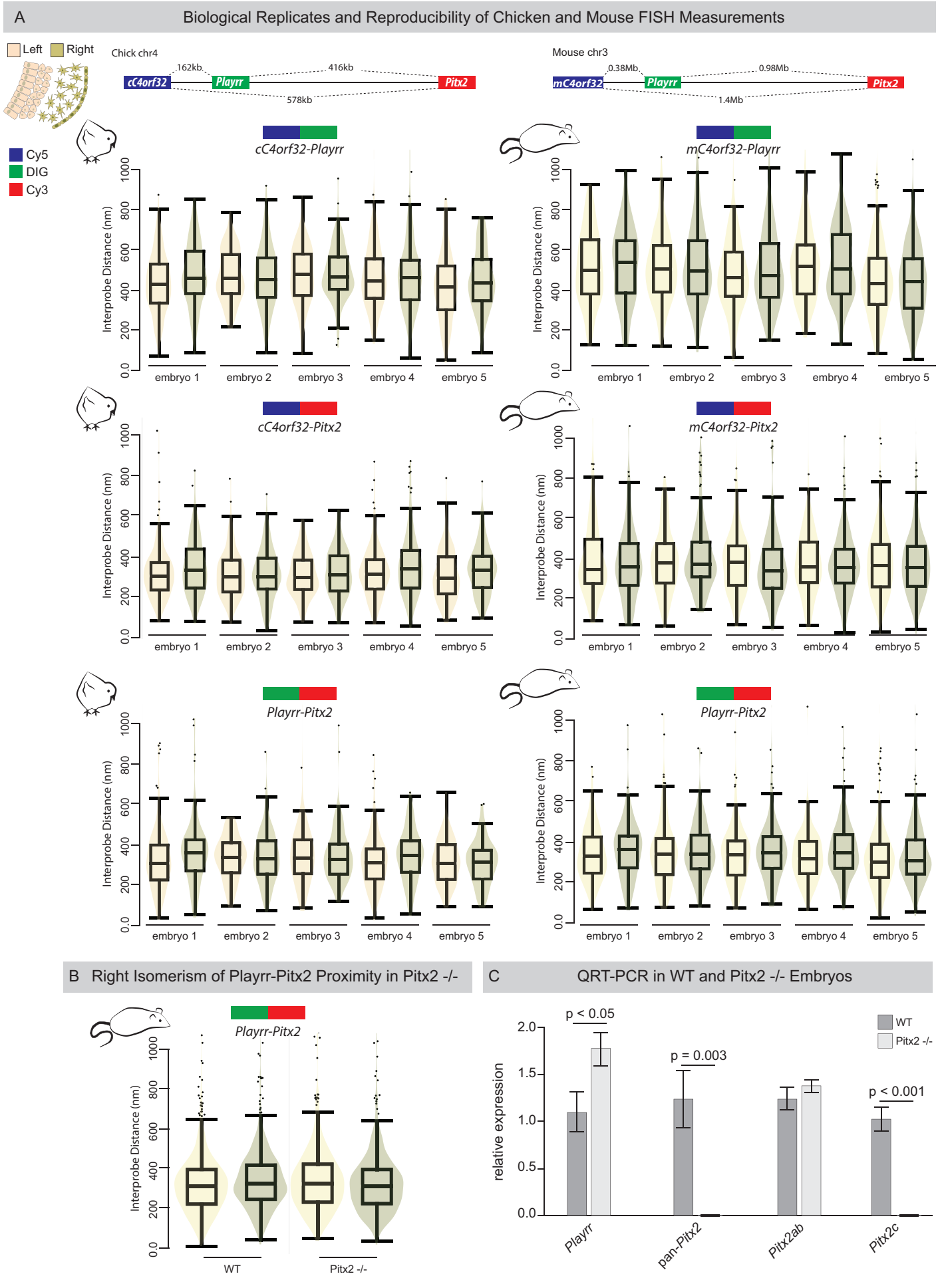
A
Biological Replicates and Reproducibility of Chicken and Mouse FISH Measurements
Left
Right
Cy5
DIG
Cy3
Chick chr4
cC4orf32
Playrr
Pitx2
162kb
416kb
578kb
Mouse chr3
mC4orf32
Playrr
Pitx2
0.38Mb
0.98Mb
1.4Mb
cC4orf32-Playrr
mC4orf32-Playrr
cC4orf32-Pitx2
mC4orf32-Pitx2
Playrr-Pitx2
Playrr-Pitx2
Interprobe Distance (nm)
0.0
200
400
600
800
1000
embryo 1
embryo 2
embryo 3
embryo 4
embryo 5
B
Right Isomerism of Playrr-Pitx2 Proximity in Pitx2 -/-
Playrr-Pitx2
Interprobe Distance (nm)
WT
Pitx2 -/-
C
QRT-PCR in WT and Pitx2 -/- Embryos
relative expression
0.0
0.5
1.0
1.5
2.0
p < 0.05
p = 0.003
p < 0.001
WT
Pitx2 -/-
Playrr
pan-Pitx2
Pitx2ab
Pitx2c

Welsh_FigS5

Cumulative Frequency Curves of Chicken and Mouse FISH Measurements

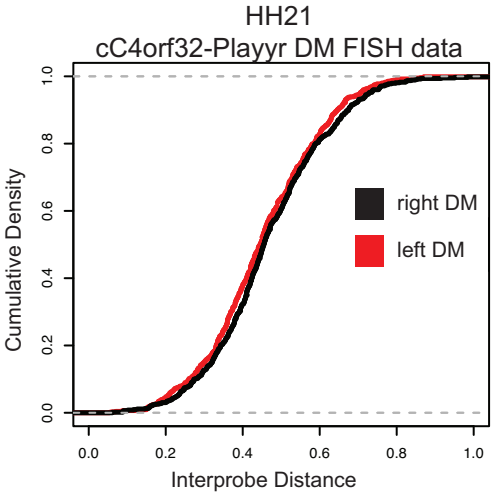

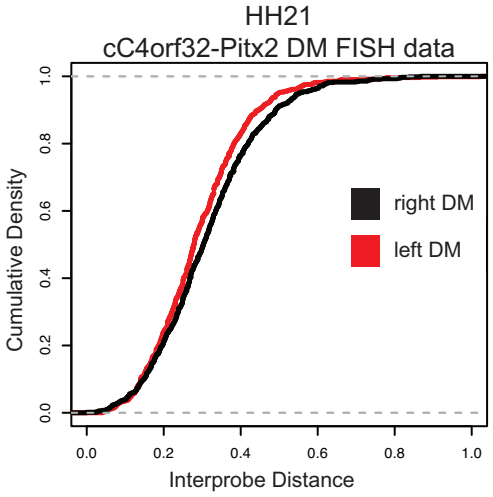

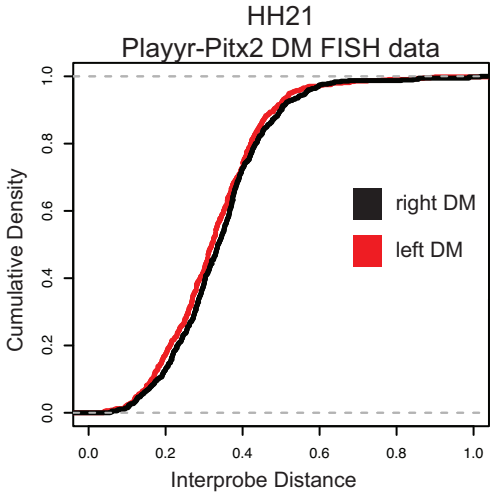

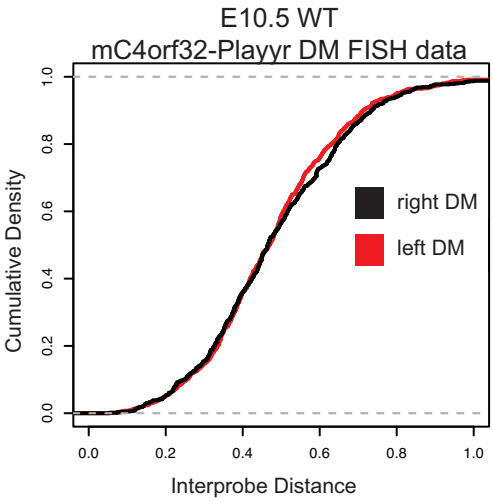

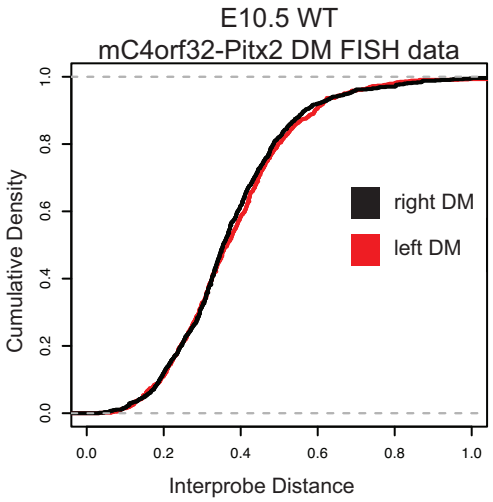

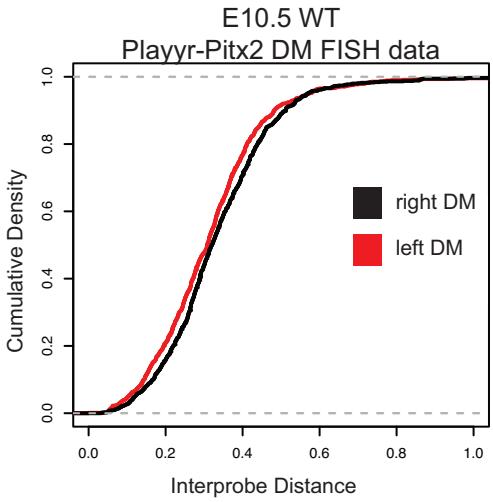

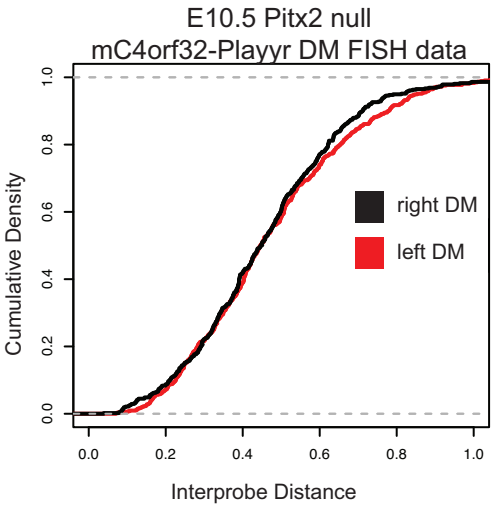

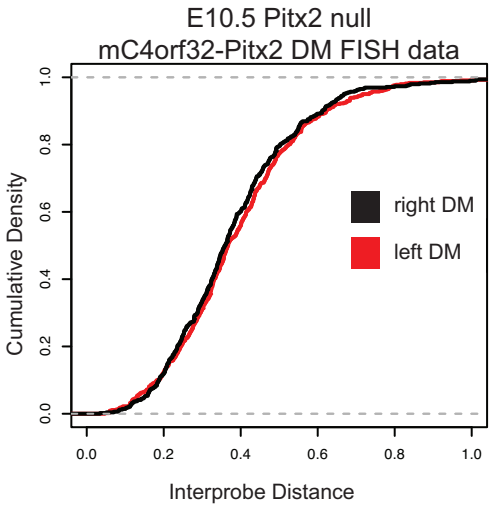

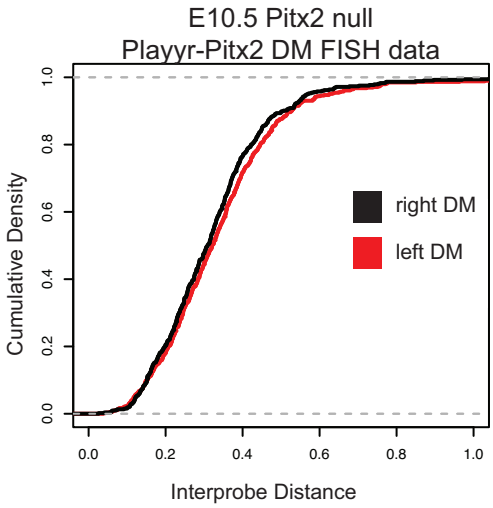

A Divergent Chick vs. Mouse Expression

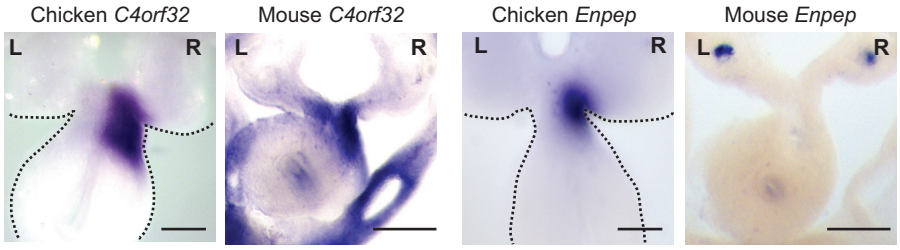

B Summary: Global, Species-specific, and Asymmetric Locus Topology

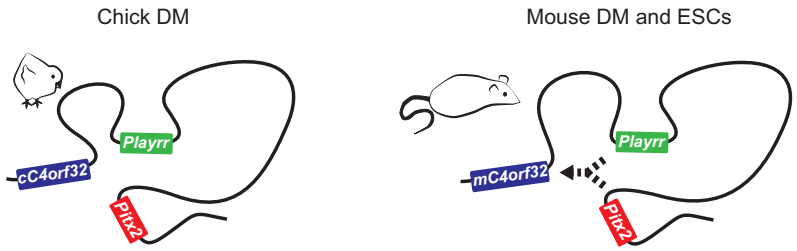

Conserved Looping Across Proximal-Distal Desert In Diverse Cell Types
and Shift in Relative Position of *mC4orf32*

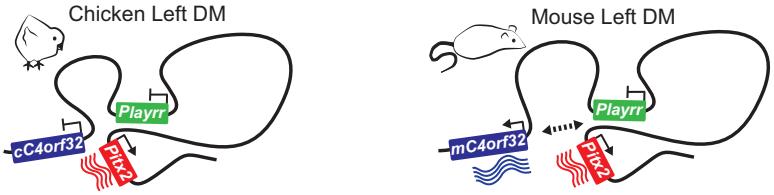

Increased Proximity
cC4orf32 OFF

Increased Separation
mC4orf32 ON

C Reduced Conservation of Proximal End of Pitx2 Locus

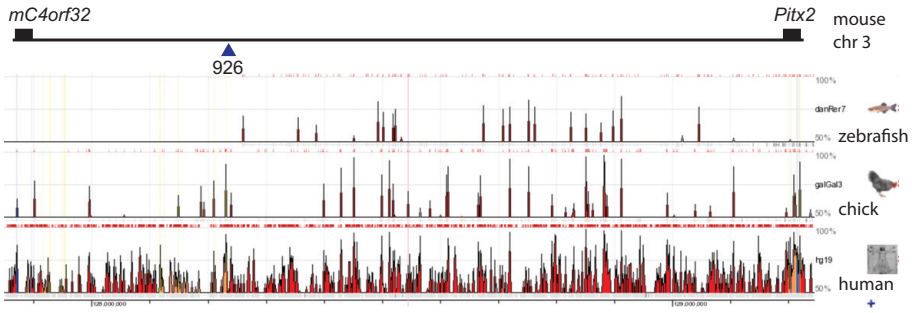

Welsh_FigS7

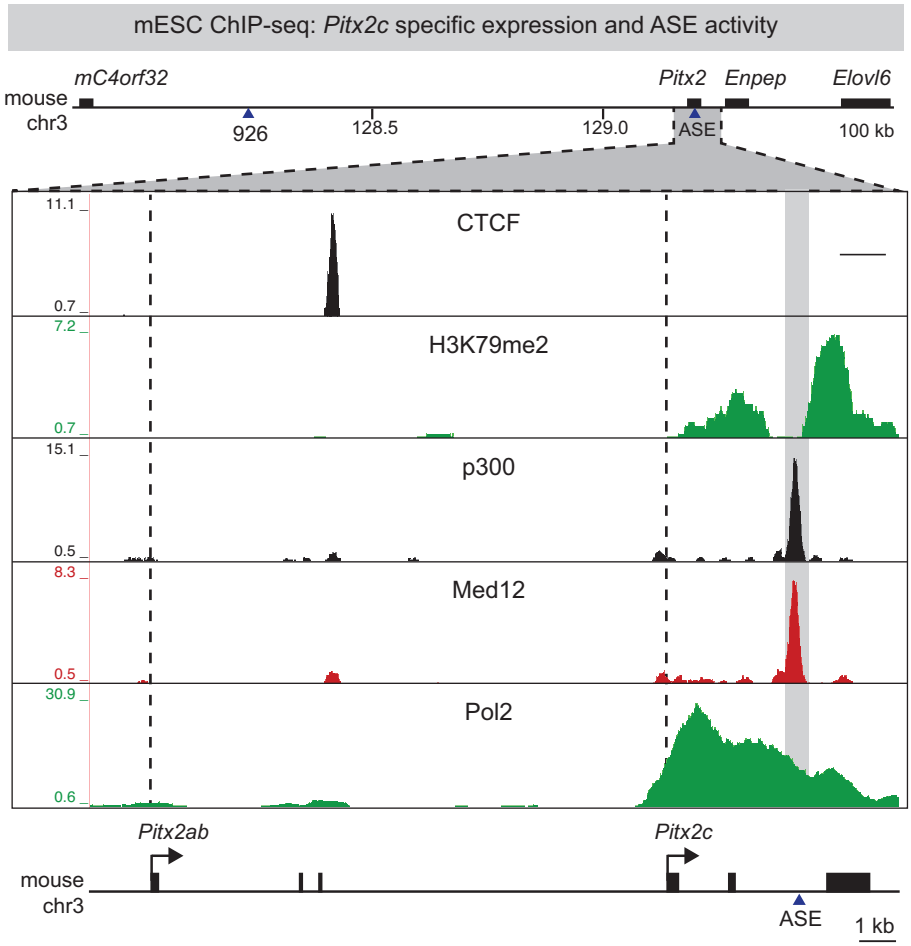
mESC ChIP-seq: *Pitx2c* specific expression and ASE activity
mC4orf32
Pitx2
Enpep
Elovl6
mouse
chr3
926
128.5
129.0
ASE
100 kb
11.1
0.7
CTCF
7.2
0.7
H3K79me2
15.1
0.5
p300
8.3
0.5
Med12
30.9
0.6
Pol2
Pitx2ab
Pitx2c
mouse
chr3
ASE
1 kb

Supplemental Figure Legends

Figure S1. Reproducible domains of asymmetric enhancer activity of hs926 by in vivo transgenic analysis. Related to Figure 1 and 3. (A) Human hs926 sequence cloned into the Hsp68-LacZ reporter construct (top) shows reproducible enhancer activity in asymmetric domains of transgenic embryos (bottom). Scale bar 100μm (B) Prediction of *Pitx2* binding sites within e926 conserved between human and mouse (top) or human and chicken (bottom) (http://rvista.dcode.org/).

Figure S2. Annotation of asymmetric *Pitx2* locus transcription in vivo using GRO-seq. Related to Figure 2. (A) GRO-seq of HH21 whole embryo characterizes nascent transcription across the *Pitx2* locus. (B) Whole embryo, HH12 head, and HH12 left & right hemisected samples were collected in addition to HH21 left and right DM samples to monitor enrichment and specificity of asymmetric transcription. (C) Transcription of bilaterally expressed *Pitx2ab* isoforms is observed in HH21 whole embryo and HH12 head. Elevated *Pitx2* expression is observed in the HH12 left hemisected sample compared to the right, while only the left DM sample detects exclusive *Pitx2c* expression. Dashed vertical lines mark *Pitx2ab* and *Pitx2c* TSS.

Figure S3. Annotation of active regulatory elements at the *Pitx2* locus in vivo using dREG. Related to Figure 2. Top: dREG annotation of the *Pitx2* locus from GRO-seq of HH21 whole embryo sample identifies a considerable number of distal regulatory elements distributed across the gene desert in addition to peaks more closely associated with coding genes. Bottom: dREG peaks in the left DM sample demonstrates enrichment

of asymmetric *Pitx2c* specific peaks and in the right DM shows absence of ASE activity. Dashed vertical lines mark *Pitx2ab* and *Pitx2c* TSS; grey box marks the ASE.

Figure S4. Reproducible L-R differences in chicken and mouse FISH data. Related to Figure 4 and 5. (A) Increased proximity in the left DM between *cC4orf32-Pitx2* and *Playrr-Pitx2* in chicken, or *Playrr-Pitx2* in mouse, is reproducible across biological replicates. Box plots show the lower quartile, median, upper quartile, and whiskers show ±1.5 times the interquartile range. Contour plotting the density of the underlying distribution of the data are color coded for left (tan) and right (green) DM. (B) Box plots showing *Playrr-Pitx2* interprobe distances in the left DM of *Pitx2* -/- embryos is indistinguishable from the right DM of WT embryos. (C) TaqMan QRT-PCR of *Playrr* and *Pitx2* isoform expression levels in *Pixt2* -/- (n=3) compared to WT (n=3), error bars ± S.E.M.

Figure S5. Cumulative density curves of chicken and mouse FISH data. Related to Figure 4 and 5. Empirical cumulative distribution frequency (ECDF) plots generated in R show cumulative density (y-axis) of FISH interprobe distance (x-axis) for each probe pair in the left or right DM measured in chicken and mouse.

Figure S6. Conserved and divergent features of the *Pitx2* locus in chicken and mouse. Related to Figure 4, 5, and 6 (A) Increased separation of *mC4orf32* from *Playrr* and *Pitx2* in mice (compare Fig. 4 and 5), and TAD structure of the *Pitx2* locus in mESCs (Fig. 6) showing that *Pitx2* and *Enpep* are positioned within separate regulatory domains is accompanied by divergent chicken vs. mouse *C4orf32* and *Enpep* DM expression. Scale bars, 100μm (B) Summary models of conserved and divergent locus topology. (C)

Comparison of conserved sequences from the mouse *Pitx2* locus with zebrafish, chicken, and human, supports that evolutionary divergence is greatest at the proximal end of the gene desert. Note that Zebrafish lack orthologs of *C4ORF32*, e926/*Playrr,* and *ENPEP*.

Figure S7. ChIP-seq analysis of mouse embryonic stem cells (mESCs). Related to Figure 6. RNA Pol II ChIP-seq data demonstrate that exclusive expression of the asymmetric *Pitx2c* isoform in mESCs is accompanied by binding at the ASE enhancer by positive regulators of transcriptional activation such as Med12, p300 and chromatin marks including H3K79 methylation deposited by the DOT1L transcriptional elongation complex via association with RNA Pol II.